

# Use of surface photoabsorption to analyze the optical response of GaAs(001) surfaces

Resul Eryiğit, Peter K. Marschel, and Irving P. Herman<sup>a)</sup>

Department of Applied Physics and the Columbia Radiation Laboratory, Columbia University, New York, New York 10027

(Received 26 April 1996; accepted 11 October 1996)

The dielectric functions of Ga- and As-terminated GaAs(001) surfaces are determined by using a three-layer model and experimentally available surface photoabsorption (SPA) data, and are compared to those previously obtained from reflectance-difference spectroscopy. Using the SPA-derived dielectric functions, approaches for optimizing conditions in SPA experiments for GaAs and other materials are presented. © 1997 American Vacuum Society.

[S0734-2101(97)02601-8]

## I. INTRODUCTION

The structure and properties of the GaAs(001) surface have been the subject of many studies because of its technological and scientific importance. This surface has several reconstructions during GaAs growth by molecular beam epitaxy (MBE) and metalorganic chemical vapor deposition (MOCVD), which depend on the growth conditions.<sup>1</sup> Two of the most powerful surface sensitive optical probes to be used to monitor the surface during growth and etching are reflectance-difference spectroscopy (RDS), which measures the normal-incidence optical anisotropy, and surface photoabsorption (SPA), which measures the difference of the reflectance of *p*-polarized light from two different surfaces, typically at an angle of incidence near the pseudo-Brewster angle ( $\theta_B$ ).<sup>2</sup> For example, Kamiya *et al.*<sup>3</sup> and Richter<sup>4</sup> have used RDS to study *in situ* several reconstructions of GaAs (001) surfaces prepared in ultrahigh vacuum by MBE and in ambient pressure H<sub>2</sub> by MOCVD. Kobayashi and Horikoshi<sup>5</sup> have employed SPA during flow-rate modulation epitaxy of GaAs as an *in situ* optical monitoring technique. Later, Nishi *et al.*<sup>6</sup> used SPA to characterize the GaAs surface during atomic layer epitaxy (ALE) with hydride and chloride reactants. Recently, Eng *et al.*<sup>7</sup> employed SPA to monitor the GaAs(001) surface during etching by modulated beams of HCl. Dietz *et al.*<sup>8,9</sup> have used a below-band gap version of SPA, called *p*-polarized reflectance spectroscopy (PRS), to study the epitaxy of GaP on Si.

The relative merits of RDS and SPA depend on their relative signal-to-noise ratios and the information content of their signals.<sup>6,10,11</sup> Since the *p*-polarized light used in SPA has electric field components both perpendicular and parallel to the surface, the reflected beam intensity is affected by transitions with dipole moments that are parallel and/or perpendicular to the surface. The electric field of the normally incident light used in RDS is parallel to the surface, and is therefore affected only by transitions with dipole moments with components parallel to the surface. As a result, the SPA signal carries more information than the RDS signal. However, RDS is more powerful than SPA in some respects since

it can probe a surface at any given time, while SPA can only compare a surface at different times.

The surface dielectric functions of Ga- and As-terminated GaAs(001) surfaces are derived here using the SPA data of Refs. 5 and 6, and are then used to determine the optimal experimental conditions for SPA, i.e., the optimum photon energy and angle of incidence. These dielectric functions are also used, along with the RDS data of Ref. 10, to examine the connection between the atomic and electronic structure of the surface and the SPA signal.

The SPA response is usually formulated as either  $\Delta R$ , the difference in reflectance in alternating processing cycles, or  $\Delta R/R$ , where  $R$  is the reflectance of a hypothetical perfect bulk-vacuum interface. While  $\Delta R$  is measured, normalizing by  $R$  makes the response seem larger for angles of incidence ( $\theta$ ) near  $\theta_B$  because the background signal from the underlying material is minimized. McIntyre and Aspnes<sup>12</sup> have shown that in such differential reflectance experiments  $\Delta R/R$  often peaks between 45° and the pseudo-Brewster angle. SPA experiments have often been conducted near  $\theta_B$  with this in mind.

## II. OBTAINING THE SURFACE DIELECTRIC FUNCTIONS

Several theories of the surface optical response have been developed, the most prominent ones being the three-layer model of McIntyre and Aspnes,<sup>12</sup> the generalized anisotropic three-layer model of Hingerl *et al.*,<sup>10,11</sup> the microscopic model developed by Del Sole and Fiorino,<sup>13</sup> the dipolar model by Wijers *et al.*,<sup>14</sup> and the electromagnetic model by Rashba.<sup>15</sup> Here we adopt the formulation of Ref. 10.

Consider a biaxial overlayer with thickness  $d \ll \lambda$ , where  $\lambda$  is the vacuum wavelength of the light, and dielectric-tensor components  $\epsilon_{xx}$ ,  $\epsilon_{yy}$ , and  $\epsilon_{zz}$  in the crystal coordinate system. The bulk and ambient dielectric functions are assumed to be isotropic, and will be called  $\epsilon_b$  and  $\epsilon_a$ , respectively, with  $\epsilon_a$  being real. The laboratory coordinates are defined with  $z$  perpendicular to the surface and  $x$  along the intersection of the surface and plane of incidence. The normalized differences in the reflectance between the relatively Ga-rich and As-rich surfaces are:

<sup>a)</sup>Electronic mail: iph1@columbia.edu

$$\frac{\Delta R_s}{R_s} = \Theta(\theta, \lambda) \text{Im} \left[ \frac{\delta \varepsilon_{xx} \Lambda(\alpha) + \delta \varepsilon_{yy} \Gamma(\alpha)}{\varepsilon_b - \varepsilon_a} \right] \quad (1a)$$

and

$$\frac{\Delta R_p}{R_p} = \Theta(\theta, \lambda) \text{Im} \left[ \frac{[\delta \varepsilon_{xx} \Gamma(\alpha) + \delta \varepsilon_{yy} \Lambda(\alpha)] [\varepsilon_b - \varepsilon_a \sin^2 \theta] - \delta \varepsilon_{zz}^{-1} \varepsilon_b^2 \varepsilon_a \sin^2 \theta}{(\varepsilon_b - \varepsilon_a)(\varepsilon_b \cos^2 \theta - \varepsilon_a \sin^2 \theta)} \right] \quad (1b)$$

for  $s$ - and  $p$ -polarized light, respectively, incident at an angle  $\theta$  to the surface normal, where  $\Delta R_{s(p)} = (R_{s(p)})_{\text{Ga}} - (R_{s(p)})_{\text{As}}$ ,  $\Theta(\theta, \lambda) = (8\pi d \sqrt{\varepsilon_a} \cos \theta) / \lambda$ ,  $\delta \varepsilon_{ii} = (\varepsilon_{ii})_{\text{Ga}} - (\varepsilon_{ii})_{\text{As}}$ ,  $\Gamma(\alpha) = (1 + \cos 2\alpha) / 2$ , and  $\Lambda(\alpha) = (1 - \cos 2\alpha) / 2$ .  $\alpha$  is the Eulerian angle between the  $x$ -axis

of the film and the laboratory, and the subscripts refer to the polarization of the incident and reflected beams.

The ‘‘differential’’ surface dielectric functions ( $\delta \varepsilon_{ii}$ ) for GaAs(001) are determined using Eqs. (1a) and (1b) by a non-linear least-squares fitting procedure to the SPA data from Refs. 5 and 6 that were obtained during the ALE of GaAs with  $\text{Ga}(\text{CH}_3)_3$  and  $\text{AsH}_3$  at nearly the same growth temperature. Specifically, data from Ref. 5 taken at  $\theta = 70^\circ$  for  $s$ - and  $p$ -polarizations at  $x$  ( $[1\bar{1}0]$ ) and  $y$  ( $[110]$ ) azimuths (substrate temperature;  $T_s = 560^\circ\text{C}$ ), and Ref. 6 taken at  $\theta = 75^\circ$  for  $p$ -polarization at  $x$  and  $y$  azimuths ( $T_s = 520^\circ\text{C}$ ) are used to obtain  $\delta \varepsilon_{xx}$ ,  $\delta \varepsilon_{yy}$ , and  $\delta \varepsilon_{zz}$ . The dielectric function of bulk GaAs ( $\varepsilon_b$ ) at  $540^\circ\text{C}$  is obtained from the seven harmonic oscillator model<sup>16</sup> and is used in Eqs. (1a) and (1b). The effective surface layer thickness  $d$  is taken to be  $2.7 \text{ \AA}$  for both Ga and As terminated layers [which corresponds to a GaAs layer in the (001) direction]. The resulting real and imaginary parts of the differential surface dielectric function components  $\delta \varepsilon_{ii}$  ( $ii = xx, yy, zz$ ) are shown in Figs. 1(a) and 1(b), respectively. The diagonal components of the dielectric function of the Ga- and As-rich surfaces can be obtained from  $\delta \varepsilon_{ii}$  only with additional information. If the relation between bulk and surface properties  $\varepsilon_b = [(\varepsilon_{ii})_{\text{Ga}} + (\varepsilon_{ii})_{\text{As}}] / 2$  is assumed, where  $ii$  is  $xx, yy, \text{ or } zz$ , the resulting surface dielectric functions are suspect because  $\varepsilon_{zz}'' < 0$  below  $2.45 \text{ eV}$ , probably because this is a poor assumption. (While this relationship with  $\varepsilon_b$  is probably somewhat more appropriate for the  $xx$  and  $yy$  components, it is still only approximate.) Only differential surface dielectric functions are needed to analyze SPA monitoring.

The six combinations of incident angles, polarizations, and incident azimuths obtainable from Refs. 5 and 6 are the minimum number of parameters required to obtain the  $\delta \varepsilon_{ii}$ 's. Error analysis was conducted to determine the sensitivity of the surface dielectric functions to experimental parameters, with the angle of incidence assumed to be the most uncertain parameter. The results are almost unchanged if a  $\pm 2^\circ$  uncertainty in  $\theta$  is assumed in the experiments reported in Ref. 5, while the same uncertainty in the data of Ref. 6 changes the magnitude of the  $\delta \varepsilon_{ii}$ 's by up to 10% with no significant change in the functional form.

More precisely, the data obtained from these six sets of experimental conditions form the minimum data set needed to determine the  $\delta \varepsilon_{ii}$ 's from the approximate expressions Eqs. (1a) and (1b), which are obtained from the exact expressions for the reflectance of a three-layer structure by keeping the first order  $d/\lambda$  term. Use of the exact expressions to find the  $\delta \varepsilon_{ii}$ 's would require the use of data from 12 experiments

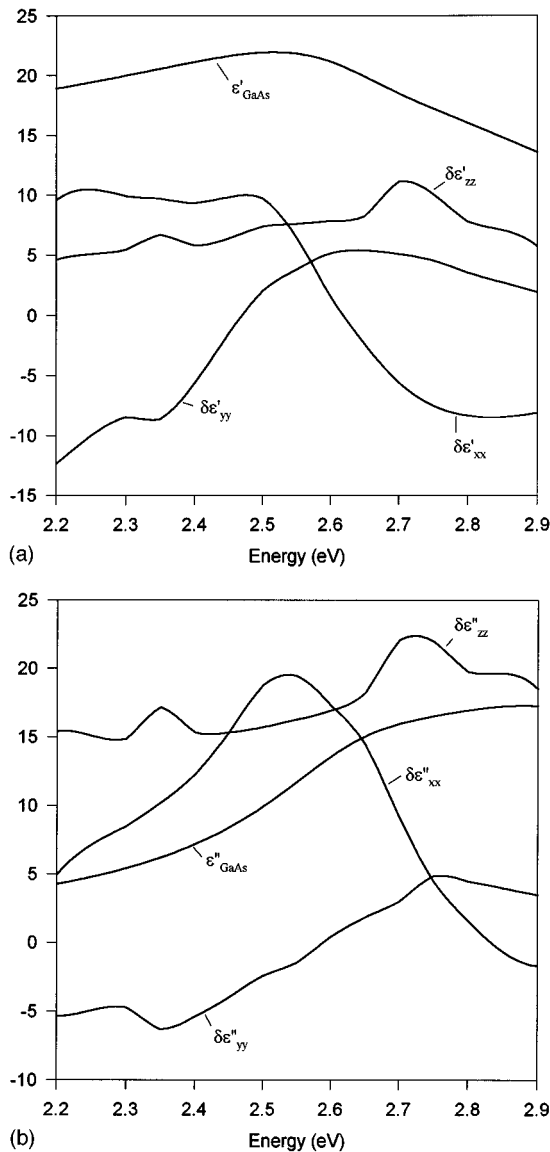


FIG. 1. (a) Real ( $\delta \varepsilon'$ ) and (b) imaginary ( $\delta \varepsilon''$ ) parts of the  $xx$ ,  $yy$ , and  $zz$  components of the differential surface dielectric function of the GaAs(001) surface, along with the response of bulk GaAs ( $540^\circ\text{C}$ ).

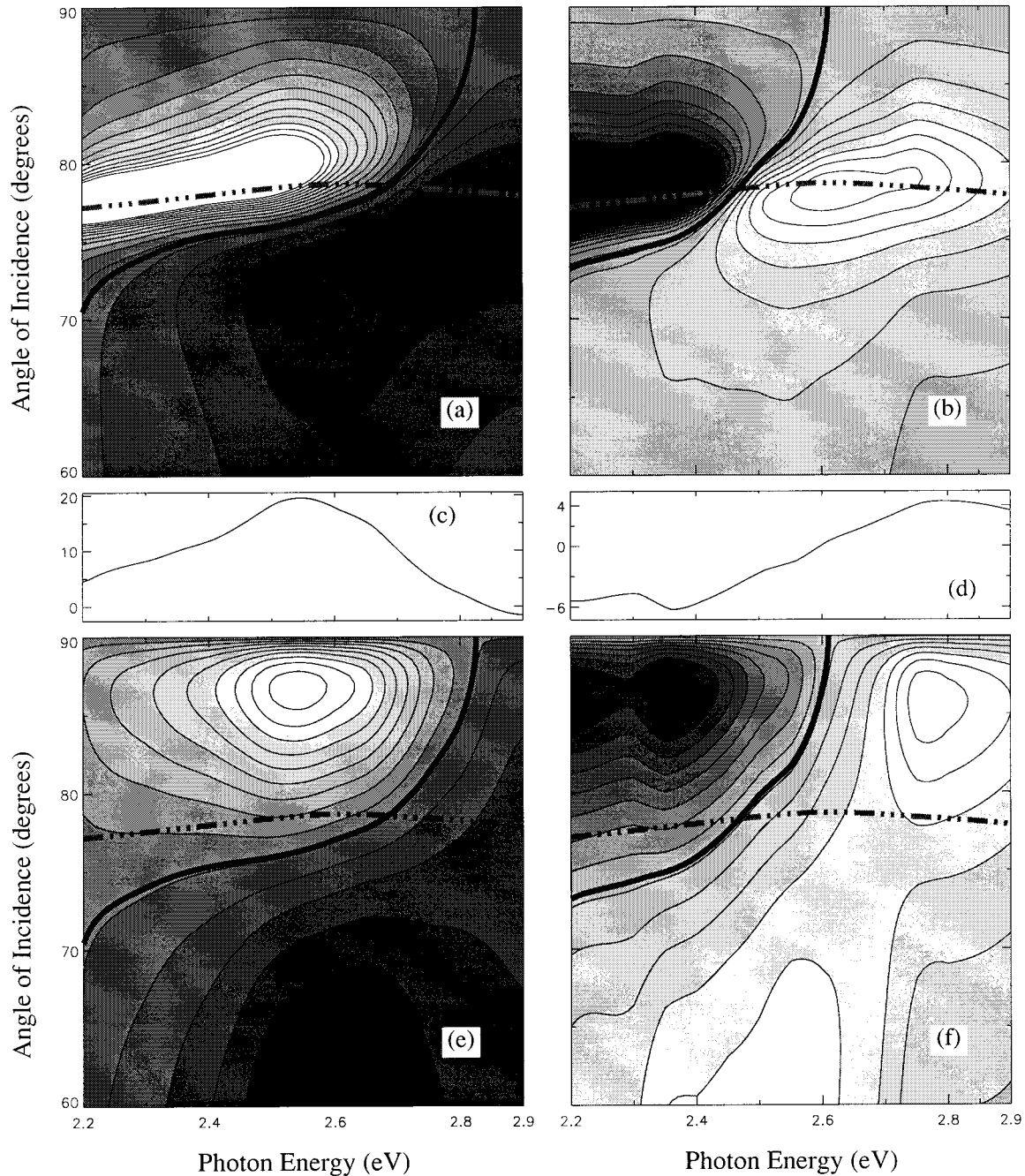


FIG. 2. Contour plots of the calculated (a)  $\Delta R_p/R_p$  (x-azimuth), (b)  $\Delta R_p/R_p$  (y-azimuth), (c)  $\text{Im}[\delta\epsilon_{xx}]$ , (d)  $\text{Im}[\delta\epsilon_{yy}]$ , (e)  $\Delta R_p$  (x-azimuth), (f)  $\Delta R_p$  (y-azimuth). The thick solid lines in (a), (b), (e), and (f) are the 0.0 contours, while the thick dash-dotted lines represent the pseudo-Brewster angle of GaAs at 540 °C. In (a), (b), (e), and (f), the black section is the most positive value and the white is the most negative, and between them there are 15 contours with equally spaced values of  $\Delta R_p/R_p$  and  $\Delta R_p$ . The maximum value, maximum contour value, spacing between contours, minimum contour value, and minimum value are: (a) [0.030, 0.025, 0.0067, -0.070, and -0.144], (b) [0.164, 0.023, 0.0042, -0.028, and -0.032], (e) [ $3.65 \times 10^{-3}$ ,  $2.81 \times 10^{-3}$ ,  $5.40 \times 10^{-4}$ ,  $-4.80 \times 10^{-3}$ , and  $-5.15 \times 10^{-3}$ ], and (f) [ $1.99 \times 10^{-3}$ ,  $1.78 \times 10^{-3}$ ,  $2.2 \times 10^{-4}$ ,  $-1.37 \times 10^{-3}$ , and  $-1.52 \times 10^{-3}$ ].

(which are not currently available)—and this would determine the surface dielectric functions for both the Ga- and As-rich surfaces—or conditions that interrelate the 12 components of the dielectric functions, such as those described above. Even though  $d/\lambda$  is very small ( $\sim 10^{-4}$ ), the values of  $\Delta R/R$  calculated using the exact and linear approxima-

tions can be quite different in some circumstances, especially near the pseudo-Brewster angle. Dietz and Bachmann<sup>9</sup> used a four layer model—with a film upon the substrate—to analyze the PRS signal obtained during GaP on Si heteroepitaxy and found that the  $\Delta R/R$  calculated with the exact and linear approximation expressions can differ by more than 20%, de-

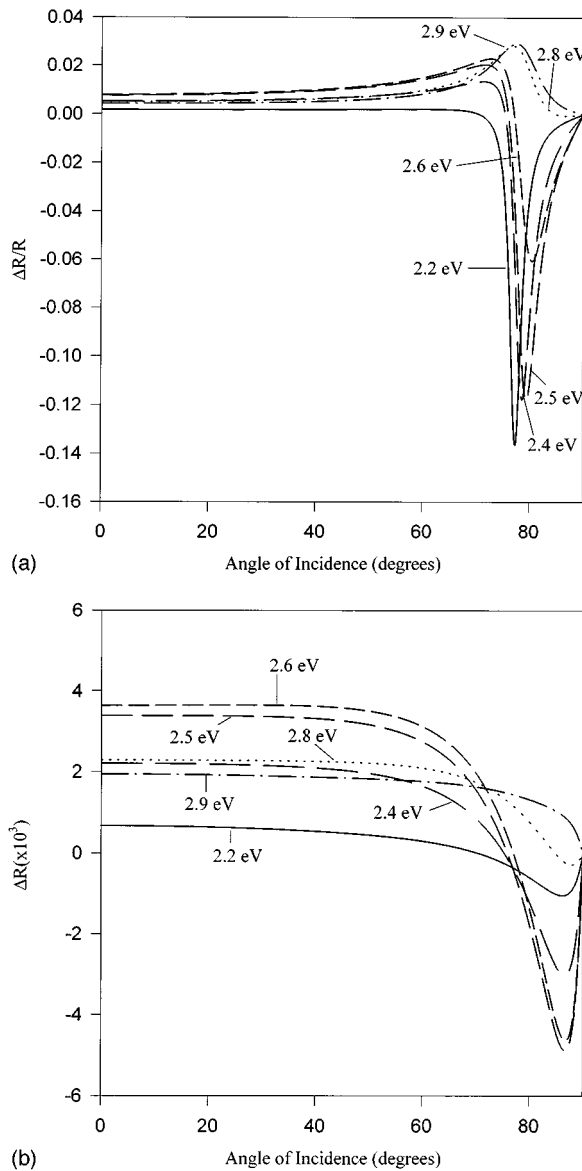


FIG. 3. The dependence of (a)  $\Delta R_p/R_p$  and (b)  $\Delta R_p$  on the angle of incidence at different photon energies [GaAs(001),  $x$ -azimuth, 540 °C].

pending on the angle of incidence and dielectric functions of the substrate and the film (for weakly or non-absorbing surfaces). For SPA, where the surface layers often absorb strongly, this difference can still strongly depend on the exact surface dielectric functions that are used, as well as the angle of incidence and the magnitude of the substrate dielectric function. For example, the difference between the value of  $\Delta R/R$  obtained here for GaAs using the approximate Eq. (1b), calculated with the “differential” surface dielectric functions ( $\delta\varepsilon_{ii}$ ), and the exact expression, calculated from the difference of  $R$  from two three-layer models (one for the Ga-rich surface and one for As-rich surface, using the  $(\varepsilon_{ii})_{\text{Ga}}$  and  $(\varepsilon_{ii})_{\text{As}}$  obtained from  $\delta\varepsilon_{ii}$  and  $\varepsilon_b = [(\varepsilon_{ii})_{\text{Ga}} + (\varepsilon_{ii})_{\text{As}}]/2$ ) is less than 8% when  $\theta$  differs from  $\theta_B(E)$  by 0.5° or more. (At the pseudo-Brewster angle of the substrate, this difference is  $\sim 18\%$ .) At the angles used

to obtain the SPA data used here, the difference is less than 5% (70°) and 7% (75°). The linear approximation is used throughout this article; this should not affect any of the main conclusions obtained here.

### III. OPTIMIZING THE SPA RESPONSE FOR GaAs AND OTHER MATERIALS

#### A. GaAs

Figure 2 shows the expected SPA response ( $\Delta R/R$  and  $\Delta R$  for  $p$ -polarized light) for GaAs(001) ALE as a function of  $\theta$  and photon energy  $E$ , using the  $\delta\varepsilon_{ii}$ 's obtained above. At a given  $E$ ,  $|\Delta R/R|$  peaks just above or below  $\theta_B$ , depending on the azimuth and photon energy, and can change by a factor of two with a half degree change in  $\theta$  near  $\theta_B$ . In contrast,  $\Delta R$  has an extremum near grazing angle, as is also seen in infrared reflection-absorption spectroscopy (IRRAS).<sup>17</sup> For GaAs this occurs at 87° near 2.55 eV for the  $x$ -azimuth, and near 2.35 eV (and 2.77 eV for the smaller magnitude extremum) for the  $y$ -azimuth. These effects are clearly observed in Fig. 3, which presents the explicit dependence of  $\Delta R/R$  and  $\Delta R$  on  $\theta$  for different  $E$ . At a given photon energy,  $\Delta R/R$  and  $\Delta R$  vary little for  $\theta < 60^\circ$ , as is seen in Fig. 3 for the  $x$ -azimuth [and is not explicitly shown in Figs. 2(a), 2(b), 2(e), and 2(f)]. At 2.55 eV, while the  $x$ -azimuth  $|\Delta R|$  attains an extremum near grazing incidence,  $|\Delta R|$  is only slightly smaller from 0° to 60°.

Figure 2 also displays the imaginary parts of the calculated “differential” surface dielectric function components  $\delta\varepsilon_{xx}$  and  $\delta\varepsilon_{yy}$  for comparison with  $\Delta R/R$  and  $\Delta R$ . It is seen that near grazing angle  $\Delta R$  has an extremum and there is a rough correspondence between the structure in  $\text{Im}[\delta\varepsilon_{xx}]$  and  $\Delta R$  for the  $x$ -azimuth ( $\sim 2.55$  eV) and between  $\text{Im}[\delta\varepsilon_{yy}]$  and  $\Delta R$  for the  $y$ -azimuth ( $\sim 2.3$  and 2.75 eV).  $\Delta R/R$  does not show a similar correspondence. At a given  $\theta$ ,  $\Delta R/R$  peaks at the  $E$  where  $R$  is minimum, which is usually where  $\text{Im}[\varepsilon_b]$  is minimum. As can be seen from Eq. (1b), the SPA signal depends on the dielectric functions of surface and the bulk in a rather convoluted way, especially if  $\varepsilon_b$  is complex. By and large, regions in  $\theta$ - $E$  parameter space where  $\Delta R/R$  and  $\Delta R$  are positive for the  $x$ -azimuth are negative for the  $y$ -azimuth, and *vice versa*. This suggests that the arrangement of the atoms on the surface after the Ga (ALE) deposition step is approximately perpendicular to that after the As deposition step.

#### B. General systems

More general conclusions can be drawn about optimizing the magnitude of the SPA response  $\Delta R_p$  and analyzing this response to determine the “differential” surface dielectric function  $\delta\varepsilon$  by using hypothetical bulk and surface dielectric functions. Figure 4 shows two rather simple cases where the bulk  $\varepsilon_b$  and surface  $\delta\varepsilon$  are modeled as single harmonic oscillators with different resonance frequencies. The  $xx$ ,  $yy$ , and  $zz$  components of  $\delta\varepsilon$  are assumed to be equal.  $\Delta R$  reaches an extremum near grazing incidence and the main “structure” of  $\Delta R$  near grazing incidence follows that of

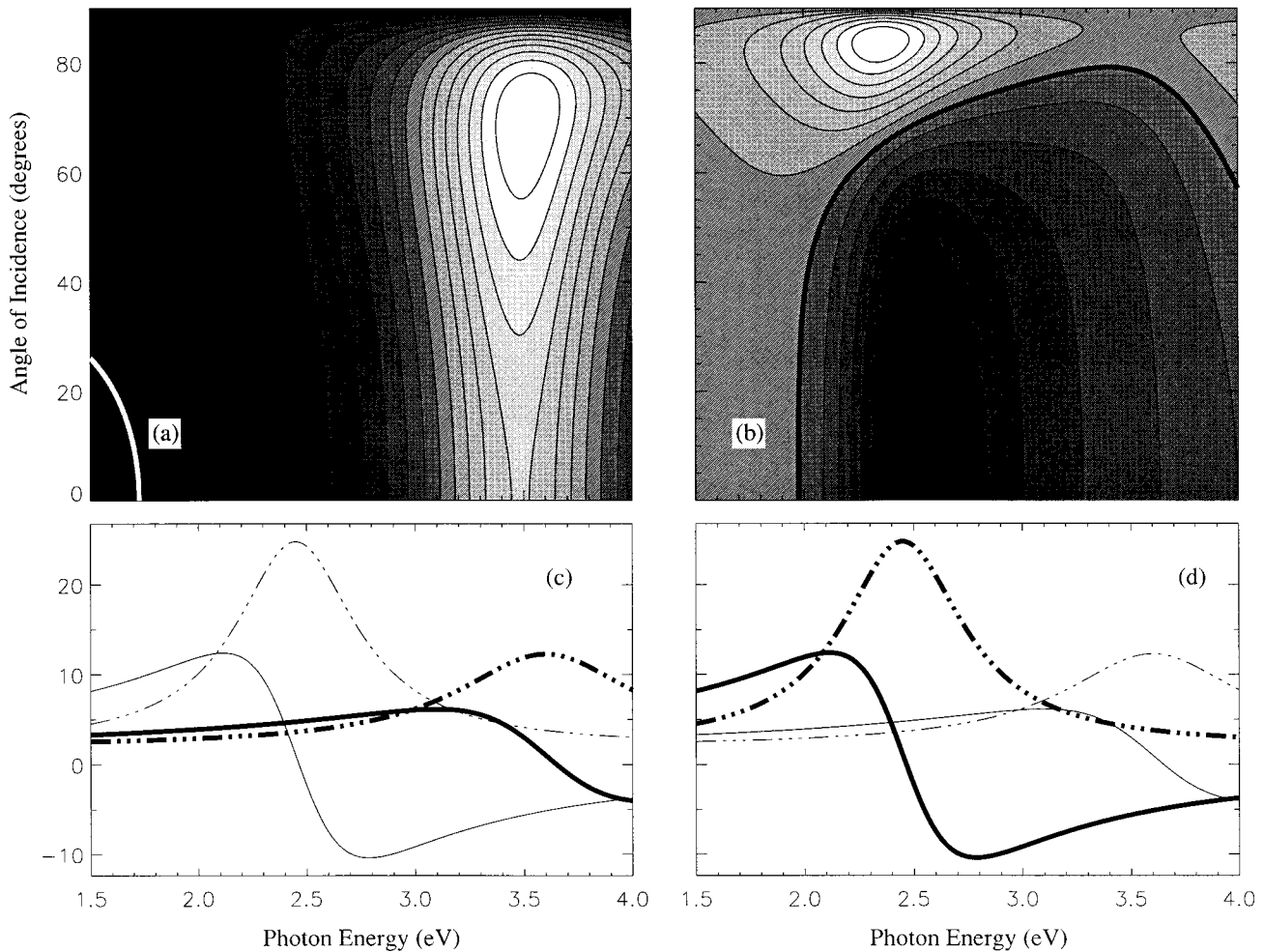


FIG. 4.  $\Delta R_p$  in (a) and (b) as a function of photon energy and angle of incidence for the “simple,” single oscillator bulk and differential surface dielectric functions shown in (c) and (d), respectively. Parts (a) and (b) have 15 equidistant contours in the interval [0.00008 (black)-(-0.02561) (white)] and [0.0104 (black)-(-0.0121) (white)], respectively. The thick solid lines in (a) and (b) are the 0.0 contours. In (c) and (d), the solid lines are the real and the dot-dashed lines are the imaginary parts, respectively, of the bulk (thin lines) and the surface (thick lines) dielectric functions.

$\delta\epsilon$ ; the resonances in  $\epsilon_b$  have relatively little effect. In the examples shown in Fig. 5 the forms chosen for the  $\epsilon_b$ 's and  $\delta\epsilon$ 's are more physical. Specifically,  $\epsilon_b$  is that of GaAs and the  $\delta\epsilon$ 's are constructed by taking the difference of two “four-harmonic oscillator” model dielectric functions. As seen in Fig. 5,  $\Delta R$  can have multiple extrema and looks more complex than that with the “simple”  $\delta\epsilon$  and  $\epsilon_b$ . However, the complex and simple cases have two common features: (1) the extremum of  $\Delta R$  in  $\theta-E$  space is almost always near grazing angle [which is not obvious from Eq. (1b)] and Eq. (2) near this angle of incidence the “structure” in  $\Delta R$  approximately follows that in  $\text{Im}[\delta\epsilon]$  [which is obvious from Eq. (1b)].

In Figs. 2(e), 4(b), and 5(a), each extremum near grazing incidence has a corresponding local extremum of opposite sign at approximately the same energy, which has a value that changes little from  $0^\circ$  to about  $40^\circ$ - $60^\circ$ . Usually this shallow-angle extremum has a magnitude that is only a little smaller than that near grazing incidence, but sometimes it

can be much smaller or even a little larger. As seen in Figs. 2(f) and 4(a), there may not be a shallow-angle extremum corresponding to that near grazing incidence.

Although analysis of  $\Delta R/R$  can improve the signal-to-noise ratio vis-à-vis that of  $\Delta R$  if there is noise in the optical source, this analysis for GaAs and other general systems shows that  $\Delta R$  is more informative about the electronic structure of the surface. Most of the noise in the optical source can be removed by nulling  $\Delta R$  by subtracting a constant or variable fraction of  $R$ . Operation near the pseudo-Brewster angle minimizes the background contribution of  $R$ , but this is not always necessary, and, in fact, often does not maximize  $|\Delta R|$ . Analysis of  $\Delta R$  near grazing incidence usually gives the largest response, as well as direct information about  $\delta\epsilon$ . (Clearly  $\delta\epsilon$  can also be determined using data obtained at other angles.) Figures 2 and 3 are helpful in determining optimum working parameters in  $\theta-E$  space for SPA monitoring of GaAs, as well as “safe” operating parameters. In particular, experiments should avoid the “zero”

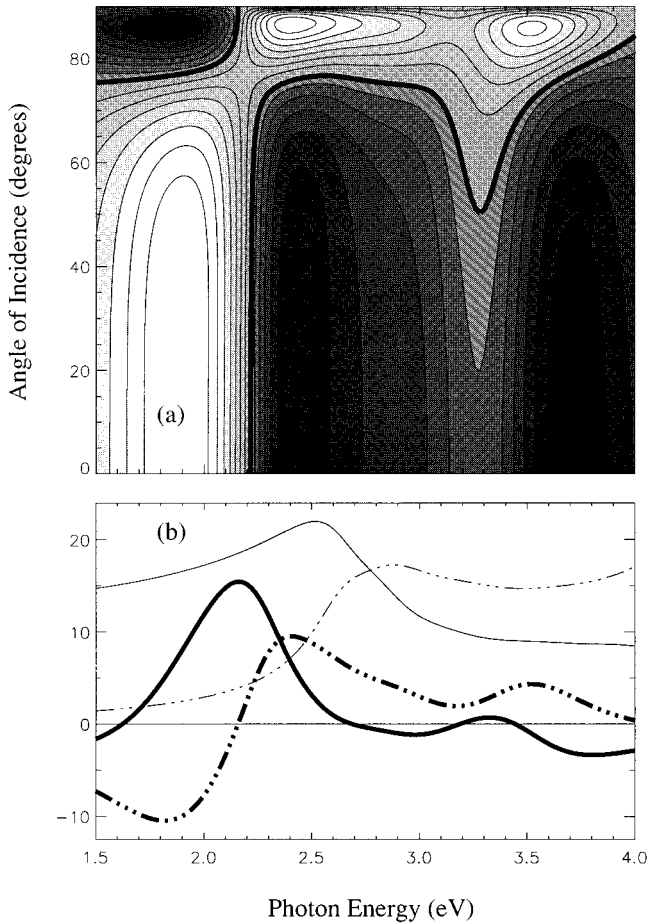


Fig. 5.  $\Delta R_p$  in (a) as a function of photon energy and angle of incidence for the bulk (GaAs at 540 °C) and “more complex” differential surface dielectric functions shown in (b). Part (a) has 15 equidistant contours in the interval [0.0022 (black)-(-0.0027) (white)]; the thick solid lines are the 0.0 contours. In (b), the solid lines are the real and the dot-dashed lines are the imaginary parts, respectively, of the bulk (thin lines) and the surface (thick lines) dielectric functions.

line and steep terraces. These figures suggest that for monitoring the GaAs surface, a shallow angle of incidence may be preferred to grazing incidence because of the need to optimize the angle of incidence near grazing angle (steep terrace).

#### IV. COMPARISON WITH RDS

The surface dielectric function information obtained from RDS and SPA monitoring of GaAs(001) epitaxy can be compared by examining the difference in various components of  $\varepsilon_{ii}$  for different surfaces. In Fig. 6, the difference in surface dielectric anisotropy  $\varepsilon_{xx} - \varepsilon_{yy}$  for different surface reconstructions (from the RDS data of Ref. 10) is compared to that determined here  $\delta\varepsilon_{xx} - \delta\varepsilon_{yy}$  from the SPA data of Refs. 5 and 6. It is seen that the  $\delta\varepsilon_{xx} - \delta\varepsilon_{yy} = (\varepsilon_{xx} - \varepsilon_{yy})_{\text{Ga}} - (\varepsilon_{xx} - \varepsilon_{yy})_{\text{As}}$  of the fitted surface dielectric functions is similar to  $(\varepsilon_{xx} - \varepsilon_{yy})_{1 \times 6} - (\varepsilon_{xx} - \varepsilon_{yy})_{c(4 \times 4)}$  of Ref. 10; it differs greatly from other  $\varepsilon_{xx} - \varepsilon_{yy}$  differences obtained using RDS (which are not shown in the figure). This would suggest

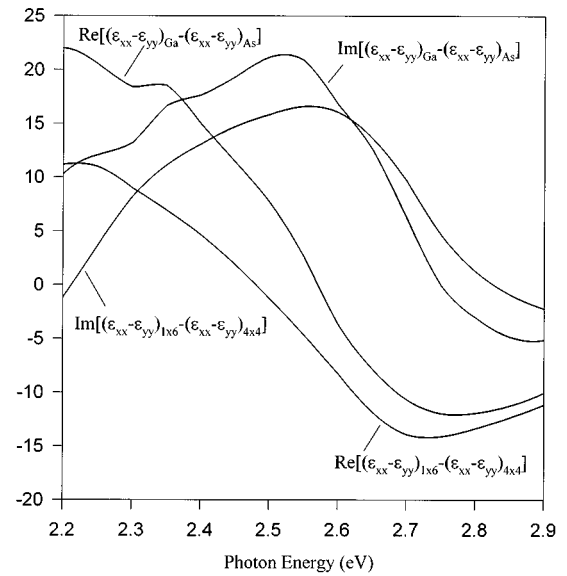


Fig. 6. The dielectric function anisotropy difference between the  $(1 \times 6)$  and  $c(4 \times 4)$  reconstructions of the GaAs(001) surface obtained from the RDS data of Ref. 10 compared with the dielectric anisotropy calculated here from SPA experiments.

that the As-rich surface observed by Nishi *et al.*<sup>6</sup> and Kobayashi and Yorikoshi<sup>5</sup> resembles the  $c(4 \times 4)$  reconstruction, while the Ga-rich surface is similar to the  $1 \times 6$  reconstruction. The  $c(4 \times 4)$  reconstruction corresponds to a surface terminated with 1.75 monolayer (ML) As, which is the common reconstruction for high As fluxes to the surface and low temperatures. The  $(1 \times 6)$  surface is a mixed (Ga and As) surface. This observation does not rule out an alternative reconstruction for the Ga- or As-terminated surfaces during ALE. The most common As- and Ga-rich surface reconstructions are the so-called missing dimer structures with 0.75 ML As and Ga coverage, respectively [ $(2 \times 4)$  and  $(4 \times 2)$  reconstructions]. The surface dielectric anisotropy obtained from SPA data seems to discount this possibility.

Kobayashi and Horikoshi<sup>5</sup> observed that at 2.6 eV  $\Delta R/R_{x\text{-azimuth}} > 0$  and  $\Delta R/R_{y\text{-azimuth}} < 0$  (for  $p$ -polarized light), which is opposite of what they expected. Their expectation seems to be based on the  $(2 \times 4)$  (As-terminated) and  $(4 \times 2)$  (Ga-terminated) reconstructions with dimers being along the  $x$  and  $y$  directions, respectively. The reconstructions deduced from Fig. 6 produce a possible explanation because on the  $c(4 \times 4)$  surface As dimerization is along the  $y$ -direction and the Ga-terminated surface is probably a  $(1 \times 6)$  surface which would have a higher response in the  $x$ -direction. [The comparison in Fig. 6 does not rule out a  $(2 \times 6)$  surface, which would be a better explanation for the observation.]

#### V. CONCLUDING REMARKS

In conclusion, available SPA data obtained during ALE are used to obtain the differential dielectric tensor of the

GaAs(001) surface, which is compared to that obtained by RDS. On the basis of this information, the optimal conditions for performing SPA monitoring are deduced. In particular, it is seen that it is better to optimize conditions for  $\Delta R_p$  rather than  $\Delta R_p/R_p$  for superior process control monitoring and evaluation of surface dielectric functions. The optimal angle of incidence may be near grazing incidence or within a broad range of shallow angles, and away from the pseudo-Brewster angle. The extrema of  $\Delta R_p$  or  $\Delta R_p/R_p$  as a function of photon energy at a given angle of incidence usually tell little about the surface dielectric function; a more complete analysis is necessary. While the specific conclusions of this study pertain only to GaAs surface, the brief analysis of other systems presented here should still help to guide the experimental design and monitoring of other surfaces with SPA.

### ACKNOWLEDGMENTS

This work was supported by NSF Grant No. DMR-94-11504 and the Joint Services Electronics Program Contract No. DAAH04-94-G-0057. The authors would like to thank T. Heinz and B. Bent for reading and commenting on this manuscript.

This work is dedicated to the memory of Professor Brian E. Bent.

- <sup>1</sup>I. Kamiya, D. E. Aspnes, L. T. Florez, and J. P. Harbison, *Phys. Rev. B* **46**, 15894 (1992), and references therein.
- <sup>2</sup>J. F. McGilp, *Prog. Surf. Sci.* **49**, 1 (1995).
- <sup>3</sup>I. Kamiya, D. E. Aspnes, H. Tanaka, L. T. Florez, J. P. Harbison, and R. Bhat, *Phys. Rev. Lett.* **68**, 627 (1992).
- <sup>4</sup>W. Richter, *Philos. Trans. R. Soc. London A* **344**, 453 (1993).
- <sup>5</sup>N. Kobayashi and Y. Horikoshi, *Jpn. J. Appl. Phys.* **29**, L702 (1990).
- <sup>6</sup>K. Nishi, A. Usui, and H. Sakaki, *Appl. Phys. Lett.* **61**, 31 (1992).
- <sup>7</sup>J. Eng, Jr., H. Fang, C. Su, S. Vemuri, I. P. Herman, and B. E. Bent, *Mater. Res. Soc. Symp. Proc.* **406**, 151 (1996).
- <sup>8</sup>N. Dietz, A. Miller, and K. J. Bachmann, *J. Vac. Sci. Technol. A* **13**, 153 (1995).
- <sup>9</sup>N. Dietz and K. J. Bachmann, *Vacuum* **47**, 133 (1996).
- <sup>10</sup>K. Hingerl, D. E. Aspnes, I. Kamiya, and L. T. Florez, *Appl. Phys. Lett.* **63**, 885 (1993).
- <sup>11</sup>K. Hingerl, D. E. Aspnes, and I. Kamiya, *Surf. Sci.* **287/288**, 686 (1993).
- <sup>12</sup>J. D. E. McIntyre and D. E. Aspnes, *Surf. Sci.* **24**, 417 (1971).
- <sup>13</sup>R. Del Sole and E. Fiorino, *Phys. Rev. B* **29**, 4631 (1984).
- <sup>14</sup>C. M. J. Wijers, R. Del Sole, and F. Manghi, *Phys. Rev. B* **44**, 1825 (1991).
- <sup>15</sup>E. I. Rashba, *J. Appl. Phys.* **79**, 4306 (1996).
- <sup>16</sup>H. Yao, P. G. Snyder, and J. A. Woollam, *J. Appl. Phys.* **70**, 3261 (1991).
- <sup>17</sup>Y. J. Chabal, *Surf. Sci. Rep.* **8**, 211 (1988).